Specific Rab GTPase-activating proteins define the Shiga toxin and epidermal growth factor uptake pathways

Evelyn Fuchs,[1] Alexander K. Haas,[1] Robert A. Spooner,[2] Shin-ichiro Yoshimura,[1,3] J. Michael Lord,[2] and Francis A. Barr[1,3]

[1]Department of Cell Biology, Max Planck Institute of Biochemistry, Martinsried 82152, Germany
[2]Department of Biological Sciences, Molecular Cell Biology Group, University of Warwick, Coventry CV4 7AL, England, UK
[3]University of Liverpool Cancer Studies Centre, Liverpool L3 9TA, England, UK

Rab family guanosine triphosphatases (GTPases) together with their regulators define specific pathways of membrane traffic within eukaryotic cells. In this study, we have investigated which Rab GTPase-activating proteins (GAPs) can interfere with the trafficking of Shiga toxin from the cell surface to the Golgi apparatus and studied transport of the epidermal growth factor (EGF) from the cell surface to endosomes. This screen identifies 6 (EVI5, RN-tre/USP6NL, TBC1D10A–C, and TBC1D17) of 39 predicted human Rab GAPs as specific regulators of Shiga toxin but not EGF uptake. We show that Rab43 is the target of RN-tre and is required for Shiga toxin uptake. In contrast, RabGAP-5, a Rab5 GAP, was unique among the GAPs tested and reduced the uptake of EGF but not Shiga toxin. These results suggest that Shiga toxin trafficking to the Golgi is a multistep process controlled by several Rab GAPs and their target Rabs and that this process is discrete from ligand-induced EGF receptor trafficking.

Introduction

Shigellosis, which is characterized by diarrhea and dysentery, is a worldwide human health problem caused by the *Shigella* group of bacteria (Niyogi, 2005). These bacteria produce a toxin, Shiga toxin, that is comprised of two components referred to as A and B, in which the A subunit is the enzymatically active toxin responsible for inactivation of the 28s ribosomal RNA, and the B subunit is required for binding and entry into target cells after transport across the polarized epithelial cells of the gut from their apical surface (for reviews see Johannes and Goud, 1998, 2000; O'Loughlin and Robins-Browne, 2001; Sandvig and van Deurs, 2002; Spooner et al., 2006). How Shiga toxin is able to enter and intoxicate cells is of great medical interest; therefore, this has been studied extensively (Sandvig et al., 1992; Mallard et al., 1998, 2002). The Shiga toxin B subunit (STxB) binds to Gb3, a neutral glycosphingolipid at the surface of target cells in the gut vasculature, as well as in the kidney and brain and is then internalized by a combination of clathrin-mediated and clathrin-independent endocytic pathways (Sandvig et al., 1989; Nichols et al., 2001; for review see O'Loughlin and Robins-Browne, 2001).

Once internalized, Shiga toxin is then transported directly from early and recycling endosomes to the trans-Golgi network (Mallard et al., 1998; Bonifacino and Rojas, 2006). This pathway is dependent on the function of clathrin and dynamin (Lauvrak et al., 2004), the small GTP-binding protein Rab6 and its effector proteins, the lipid phosphatase OCRL1, a defined set of SNAREs (Mallard et al., 2002; Monier et al., 2002; Tai et al., 2004; Choudhury et al., 2005; Hyvola et al., 2006), and a second GTP-binding protein Arl1 and its effector golgin-97 (Lu et al., 2004). From the TGN, the toxin is then transported by a retrograde pathway dependent on Rab6 through the Golgi apparatus to the ER (Sandvig et al., 1992; White et al., 1999), where the toxin A subunit enters the cytoplasm most likely by retrotranslocation (for review see Sandvig and van Deurs, 2002).

Despite the multistep nature of the Shiga toxin uptake pathway, only a single Rab GTP-binding protein, Rab6, has been shown to play any role in its transport (Girod et al., 1999; White et al., 1999; Mallard et al., 2002). Because each membrane trafficking step is thought to involve a discrete set of Rabs (Zerial and McBride, 2001), it seems likely that additional Rabs are involved in Shiga toxin uptake. To further define the pathway

Correspondence to Francis A. Barr: f.a.barr@liverpool.ac.uk

Abbreviations used in this paper: GAP, GTPase-activating protein; STxB, Shiga toxin B subunit.

The online version of this article contains supplemental material.

The Journal of Cell Biology, Vol. 177, No. 6, June 18, 2007 1133–1143
http://www.jcb.org/cgi/doi/10.1083/jcb.200612068

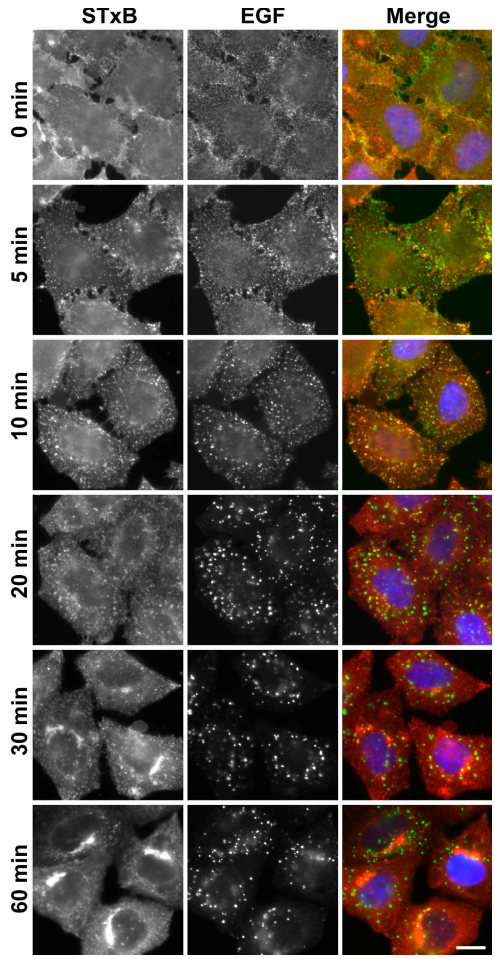

Figure 1. **Comparison of the Shiga toxin and EGF uptake pathways.** Fluorescently labeled STxB (red) and EGF (green) were bound on ice to the surface of HeLa cells starved of serum overnight. Excess ligands were washed away, and the cells were incubated in complete growth medium at 37°C for the times indicated in the figure. The cells were then fixed and mounted without further processing. DNA was stained with DAPI (blue). Bar, 10 μm.

of Shiga toxin transport between the cell surface and the Golgi apparatus, we have focused on the identification of Rab GTPase-activating proteins (GAPs) that interfere with this step. Rab GAPs are characterized by a conserved catalytic domain, the TBC (Tre2/Bub2/Cdc16) domain (Strom et al., 1993; Albert and Gallwitz, 1999; Albert et al., 1999), that promotes GTP hydrolysis by a dual arginine/glutamine finger catalytic mechanism related to the arginine finger mechanism of Ras GAPs (Ahmadian et al., 1997, 1999; Rak et al., 2000; Pan et al., 2006). As we have shown previously in the case of Rab5 (Haas et al., 2005), Rab GAPs can be used to specifically inactivate the endogenous pool of a Rab and, thus, interfere with the process this Rab is involved in. Nonspecific effects of Rab GAP expression can easily be discriminated from the specific effects of Rab inactivation by use of an inactive point mutant in which the catalytic arginine residue is replaced by alanine (Haas et al., 2005).

Because the human genome encodes >60 Rabs and at least 39 TBC domain–containing proteins, the identification of specific Rab–Rab GAP pairs is not a trivial task (Zerial and McBride, 2001; Haas et al., 2005). In the present study, we have screened for human Rab GAPs that specifically inhibit the transport of Shiga toxin to the Golgi apparatus and do not have any effects of the uptake of EGF and its receptor. By combining this functional assay with biochemical analysis of GTP hydrolysis, we are able to identify discrete pairs of Rabs and Rab GAPs acting in the Shiga toxin and EGF transport pathways.

Results

Molecular requirements for Shiga toxin and EGF trafficking

To investigate the requirements for specific Rab GAPs in the trafficking of Shiga toxin to the Golgi but not the endocytic uptake of growth factors such as EGF, it was necessary to establish conditions for the uptake of these two ligands. Fluorescently labeled STxB and EGF were bound to the cell surface on ice, and, after washing to remove excess toxin, cells were warmed, and uptake of the two ligands was followed by immunofluorescence microscopy (Fig. 1). Initially, both ligands were present on the cell surface (0 min) and became internalized into small punctate structures at 10–20 min (Fig. 1). After this, the two markers separated, and Shiga toxin accumulated in a perinuclear compartment from 30 to 60 min that was previously shown to correspond to the trans-Golgi network and Golgi stacks (Sandvig et al., 1992; Mallard et al., 1998), whereas, as expected, EGF remained in punctate endosomal structures (Fig. 1). Interestingly, although both ligands have been reported to be taken up by clathrin-dependent pathways (Sandvig et al., 1989; Nichols et al., 2001), the kinetics of uptake are clearly different, indicating that there may be some differences in the mechanistic details such as the requirement for Rab GTPases. Therefore, for further experiments, it was decided to take a 60-min uptake of Shiga toxin to measure the efficiency of its transport to the Golgi and a 30-min uptake of EGF to measure its uptake into early endosomes.

The uptake of Shiga toxin has previously been shown to be Rab6 dependent (White et al., 1999; Mallard et al., 2002), whereas that of EGF should be Rab6 independent. To verify this, the uptake of these two ligands was followed in cells depleted of Rab6 (Fig. 2). Immunofluorescence analysis showed that Rab6 was efficiently depleted after 72 h of treatment with specific siRNA duplexes (Fig. 2 A). Importantly, the Rab6 effector protein Bicaudal-D1 was redistributed from the Golgi to the cytoplasm (Fig. 2 A), indicating that Rab6 function was impaired. Compared with control cells, Rab6 depletion resulted in a decrease in the amount of Shiga toxin reaching the Golgi apparatus after 60 min of uptake (Fig. 2 B). Under these conditions, the Golgi marker TGN46 was unaltered, suggesting that this decrease is not caused by disruption of the Golgi apparatus. In contrast, no obvious differences could be seen in the uptake of EGF when comparing control and Rab6-depleted cells (Fig. 2 B). Expression of a dominant-active mutant of Rab5 resulted in the formation of enlarged early endocytic structures coated with the Rab5 effector EEA1 as expected (Stenmark et al., 1994). These structures accumulated both EGF and Shiga toxin, suggesting that these ligands traffic via a Rab5-dependent pathway through early endosomes (Fig. 2 C).

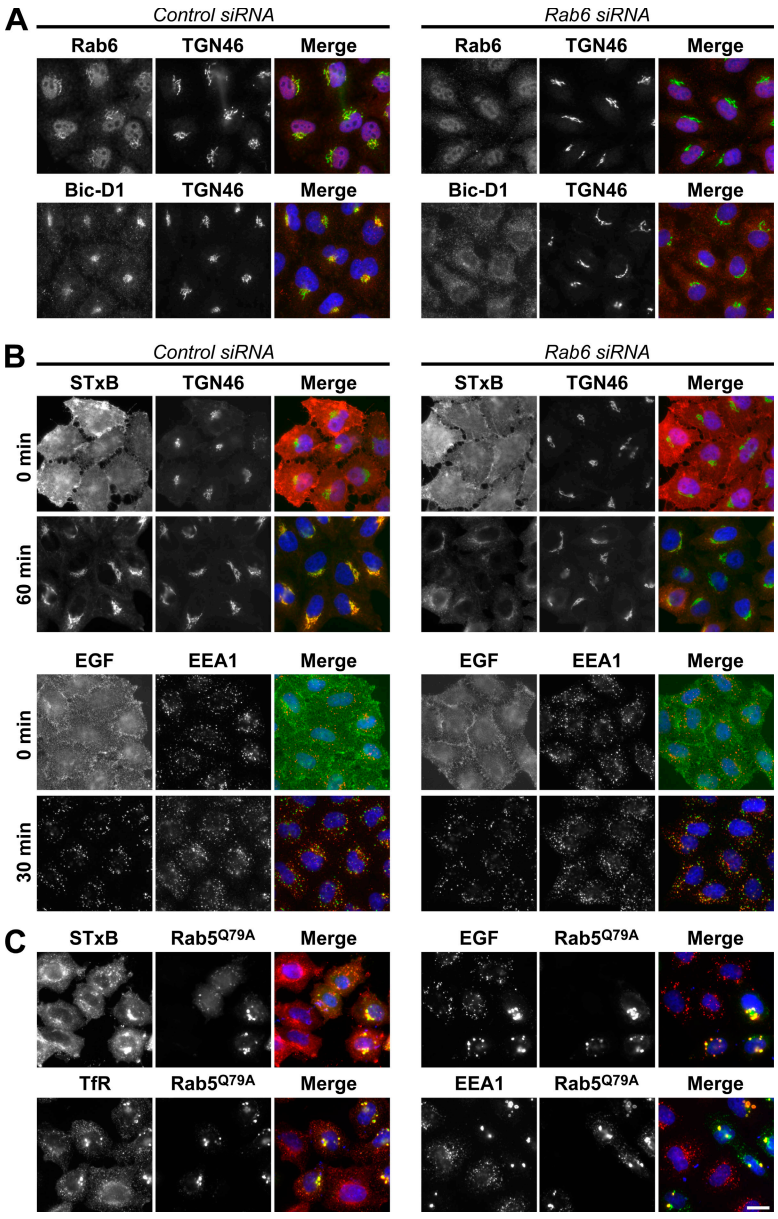

Figure 2. **Shiga toxin but not EGF uptake is Rab6 dependent.** (A and B) HeLa cells were treated with control or Rab6 siRNA for 72 h and were either fixed and stained with antibodies to either Rab6 or Bicaudal-D1 (red) and TGN46 (green; A) or used for Shiga toxin (red) and EGF (green) uptake assays and costained for TGN46 (green) or EEA1 (red; B). (C) HeLa cells transfected with the GFP-tagged $Rab5^{Q79A}$ dominant-active mutant (green) for 24 h were used for Shiga toxin and EGF (red) uptake assays or were stained for EEA1 and transferrin receptor (red). DNA was stained with DAPI (blue). Bar, 10 μm.

Therefore, EGF takes a Rab6-independent trafficking route, whereas Shiga toxin transport to the Golgi is Rab6 dependent. Based on these findings, a Rab6 GAP would be expected to block Shiga toxin but not EGF uptake, whereas a Rab5 GAP might block both. Because specific GAPs for both Rab5 and Rab6 have previously been identified (Cuif et al., 1999; Lanzetti et al., 2000; Haas et al., 2005), these predictions were tested.

Shiga toxin trafficking to the Golgi apparatus is independent of TBC1D11/GAPCenA

It has previously been reported that TBC1D11/GAPCenA is the GAP for Rab6 (Cuif et al., 1999), and, thus, this was tested for its ability to block the trafficking of Shiga toxin to the Golgi apparatus. Surprisingly, the expression of TBC1D11/GAPCenA had no obvious effect on the transport of Shiga toxin to the Golgi apparatus (Fig. 3 A) or on the ability of Rab6 or the Rab6-dependent effector Bicaudal-D1 (Matanis et al., 2002; Short et al., 2002) to target to Golgi membranes (Fig. 3 B). Therefore, TBC1D11/GAPCenA was further investigated to find out whether it has the biochemical properties expected of a Rab6 GAP.

Confirming previous findings (Cuif et al., 1999), a C-terminal fragment of TBC1D11/GAPCenA was identified when Rab6 was screened against a yeast two-hybrid cDNA library (unpublished data). However, this fragment corresponding to a predicted coiled-coil region adjacent to the GAP domain does not show a specific interaction with Rab6 and binds to human Rabs of many different subfamilies when tested against a representative collection of human Rabs (Fig. 3 C). When full-length TBC1D11/GAPCenA was tested, it showed a strong interaction with Rab4, a weaker interaction with Rab11, and only a very weak interaction with Rab6 (Fig. 3 C). A more detailed analysis in which multiple deletion constructs of TBC1D11/GAPCenA were tested revealed that regions N and C terminal to the core

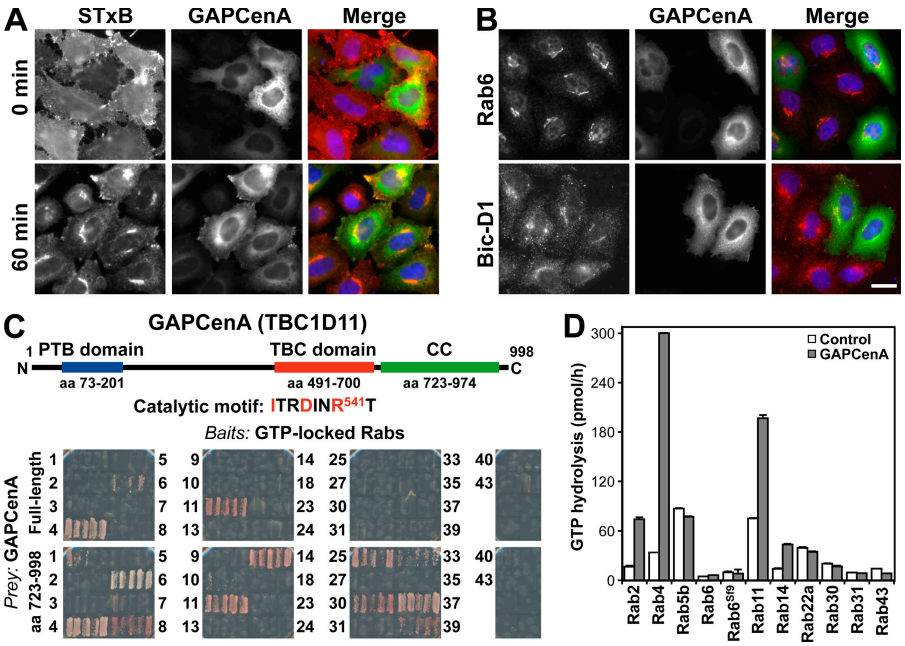

Figure 3. **TBC1D11/GAPCenA is a GAP for Rab4 and does not block Shiga toxin uptake.** (A) HeLa cells transfected with GFP-tagged TBC1D11/GAPCenA (green) were used for Shiga toxin uptake assays (red). (B) The ability of Rab6 and Bicaudal-D1 (red) to localize to the Golgi was tested in cells expressing GFP-tagged TBC1D11/GAPCenA (green). (C) A schematic of TBC1D11/GAPCenA shows the putative phosphotyrosine-binding domain (PTB; blue), the TBC domain (red), and a C-terminal coiled-coil region (green). Full-length TBC1D11/GAPCenA and the C-terminal coiled-coil region identified by unbiased yeast two-hybrid library screen prey constructs were tested against the human Rabome bait construct library as described in Materials and methods. All conditions showed equal growth on nonselective media; the ability to grow on the selective media shown in the figure is an indicator of an interaction between the bait and prey. (D) GAP assays were performed using 0.5 pmol of recombinant TBC1D11/GAPCenA (closed bars) or a buffer control (open bars) and 100 pmol of the Rabs indicated in the figure. Two preparations of Rab6 were used: one from bacteria (Rab6), and the other a prenylated preparation produced in insect cells (Rab6^{Sf9}). Error bars represent SD. Bar, 10 μm.

TBC domain contribute to the recognition of specific Rabs (Fig. S1, available at http://www.jcb.org/cgi/content/full/jcb.200612068/DC1). This suggested that Rab6 might not be the target for TBC1D11/GAPCenA after all, and biochemical assays were performed to test this. In agreement with the yeast two-hybrid data, TBC1D11/GAPCenA had strong GAP activity toward Rab4 and a lesser activity toward Rab11 (Fig. 3 D). Only very weak activity was detected toward Rab2 and 14 (Fig. 3 D), which fall into the same Rab subfamily as Rab4 and 11, showing that TBC1D11/GAPCenA can discriminate between closely related Rabs. No activity could be detected toward Rab6 or any of the other Rabs tested (Fig. 3 D), although all were loaded with GTP to the same extent. It was previously suggested that Rab6 has to be prenylated to be an efficient substrate for TBC1D11/GAPCenA, and this was tested. However, no GAP activity could be seen when prenylated Rab6 purified from insect cells was used (Fig. 3 D, Rab6^{Sf9}). It should also be noted that Rab4 was prepared in bacteria and was therefore not prenylated but was still an excellent substrate for TBC1D11/GAPCenA. These data show that TBC1D11/GAPCenA is a GAP for Rab4 but not Rab6 and that it does not alter the trafficking of Shiga toxin to the Golgi apparatus.

A screen for Rab GAPs altering Shiga toxin trafficking

An unbiased approach was taken to identify which Rab GAPs act on the Shiga toxin transport pathway. Cells expressing the various predicted human Rab GAPs were tested blindly for their ability to transport Shiga toxin to the Golgi apparatus and EGF to early endosomes (unpublished data). Candidate positives from this first round of screening were then retested, comparing the effects of the wild-type GAP to that of a catalytically inactive point mutant. In this screen, 6 of 39 predicted GAPs showed catalytic activity–dependent effects on Shiga toxin trafficking to the Golgi apparatus (Table I and Fig. 4, A and B). In contrast, in a parallel screen, only RabGAP-5 was able to block the uptake of EGF to early endosomes (Table I and Fig. 5, A and B).

To be sure that the lack of a Golgi signal for Shiga toxin after 60 min of uptake was not simply a result of disruption of the Golgi, the integrity of this organelle was tested using markers for the cis- and trans-Golgi compartments (Fig. S2, available at http://www.jcb.org/cgi/content/full/jcb.200612068/DC1). This resulted in the elimination of GAPs such as TBC1D22A and 22B in which the Golgi was fragmented, and Shiga toxin was found to localize to these fragments (Fig. S2 and not depicted). In the case of TBC1D14, although the Golgi was fragmented, Shiga toxin did not localize to these Golgi fragments, indicating there was a block in transport. However, these effects were not caused by Rab inactivation because the inactive point mutant gave a similar phenotype (Fig. 4, A and B; and Fig. S2). Interestingly, there was no effect on the trafficking of EGF, suggesting that TBC1D14 is not disrupting early endosome function. In contrast, RN-tre, although fragmenting the Golgi, caused a block of Shiga toxin in more peripheral structures discrete from the Golgi dependent on its catalytic activity; therefore, this was counted as a positive (Figs. 4 and S2, and not depicted).

The ability of candidate positives to protect cells against the cytotoxic effects of complete Shiga-like toxin 1 was then tested (Fig. 4 C). This assay measures protein synthesis, which is inhibited if Shiga toxin can reach the ER and enter the cytoplasm and, therefore, is a more stringent measure of Shiga toxin trafficking than fluorescent assays (Spooner et al., 2004). This approach showed that EVI5, RN-tre, and TBC1D17 protect against Shiga-like toxin 1 between 1.87- and 3.35-fold, whereas RabGAP-5 with a fold protection of 1.07 could not (Fig. 4 C).

Table I. **Effects of human TBC domain–containing proteins on Shiga toxin transport**

Rab GAP		Wild-type TBC domain				Catalytically inactive TBC domain		
	Target Rab	STxB	GAP localization	EGF	Golgi	STxB	GAP localization	EGF
EVI-5	35	Vesicular	Cytosolic	Early endosomes[a]	Intact	Golgi	Tubules, cytosolic	ND
RN-tre (USP6NL)	41	Cell surface vesicular	Cell surface	Early endosomes[a]	Fragmented	Golgi	Cell surface	ND
RabGAP-5 (RUTBC3)	5A-C	Golgi	Cytosolic	Cell surface	Intact	Golgi[b]	Cytosolic	Early endosomes
TBC1D10A	ND	Vesicular Golgi	Cell surface	Early endosomes[a]	Intact	Golgi	Cell surface	ND
TBC1D10B	22a/31	Vesicular	Cell surface	Early endosomes	Intact	Golgi	Cell surface	ND
TBC1D10C	ND	Vesicular	Filopodia, cell surface	Early endosomes	Intact	Golgi	Cell surface	ND
TBC1D11 (GAPCenA)	4>11	Golgi	Cytosolic	Early endosomes	Intact	ND	Cytosolic	ND
TBC1D14	ND	Recycling endosomes	Recycling endosomes	Early endosomes	Fragmented	Recycling endosomes	Recycling endosomes	ND
TBC1D17	21	Vesicular	Cytosolic	Early endosomes	Intact	Golgi	Cytosolic	ND
TBC1D22A	33A-B[c]	Golgi fragments	Cytosolic, nuclear	Early endosomes	Fragmented	Golgi	Cytosolic/ nuclear	ND
TBC1D22B	33A-B[c]	Golgi fragments	Cytosolic, nuclear	Early endosomes	Fragmented	Golgi	Cytosolic/ nuclear	ND

HeLa cells were transfected for 24 h with GFP-tagged wild-type or catalytically inactive Rab GAPs. These cells were then used for SSTxB or EGF uptake assays, and the uptake of STxB and EGF were scored at 1 h or 30 min, respectively. A 0-min time point was also taken to verify that both STxB and EGF were bound to the cell surface with equal efficiency for all conditions. Localization of the GFP-tagged Rab GAPs was also scored.
[a]Some highly expressing cells failed to bind EGF at the zero time point, indicating a potential defect in the trafficking of EGF receptor to the cell surface. However, the majority of cells bound and took up EGF as normal.
[b]The RabGAP-5 GAP domain was used for this experiment.
[c]TBC1D22 family GAPs have previously been shown to act on Rab33 (Pan et al., 2006).

The TBC1D10 family of GAPs showed variable extents of protection, and, therefore, it is unclear whether these represent specific positives with this assay. Interestingly, none of the positive GAPs were able to cause the release of the Rab6 effector Bicaudal-D1 from Golgi membranes (Fig. S3, available at http://www.jcb.org/cgi/content/full/jcb.200612068/DC1), even those that showed some effects on Golgi morphology (Fig. S2). This suggests that they do not act on Rab6. The trafficking pathway of Shiga toxin from the cell surface to the Golgi is therefore defined by the following Rab GAPs: EVI-5, RN-tre, the TBC1D10 family, and TBC1D17.

Different GAPs define the uptake routes for EGF and Shiga toxin

Although RN-tre was initially suggested to act on Rab5 and, thus, the EGF uptake pathway (Lanzetti et al., 2000), more recently, another GAP, RabGAP-5, has also been proposed to fulfill this function (Haas et al., 2005). To clarify this point, the effects of RN-tre and RabGAP-5 on the uptake of EGF and Shiga toxin were directly compared (Fig. 6). RabGAP-5 was able to block the uptake of EGF (Fig. 6 A) and displace the Rab5-dependent effector molecule EEA1 from endosomes (Fig. 6 B) but had no effect on the uptake of Shiga toxin (Fig. 6 C). RN-tre or a catalytically inactivate point mutant of RabGAP-5 did not show these effects on EGF uptake (Fig. 6, A and B). In contrast, RN-tre was able to block the transport of Shiga toxin to the Golgi apparatus (Fig. 6 C) and caused partial fragmentation of the Golgi apparatus (Figs. 6 D and S2), which is consistent with previous observations that its target, Rab43, is localized to this organelle (Haas et al., 2005). Note that Rab43 was referred to as Rab41 in a previous study (Haas et al., 2005), which is consistent with the naming in mice; however, the gene nomenclature has now been clarified so that this gene is called Rab43 in both the mouse and human. RabGAP-5 or a catalytically inactive point mutant of RN-tre did not show these effects (Fig. 6, C and D). In some cells expressing very high levels of RN-tre, the uptake of EGF was blocked, but further investigation revealed that these cells lack detectable EGF receptor on the cell surface (unpublished data). Therefore, the apparent uptake block is caused by a lack of EGF binding and not by a defect in endocytosis of the receptor–ligand complex. One explanation for the reduced level of EGF receptor at the cell surface could be the disrupted Golgi apparatus seen in RN-tre–expressing cells (Figs. 6 D and S2). Thus, any effects of RN-tre on EGF receptor uptake would appear to be indirect.

Identification and verification of target Rabs

To identify the target Rabs of the positive GAPs identified thus far, they were tested for their ability to accelerate GTP hydrolysis by a specific Rab in biochemical assays with a wide set of human Rabs (Fig. 7). These data clearly show that of the Rabs tested, the

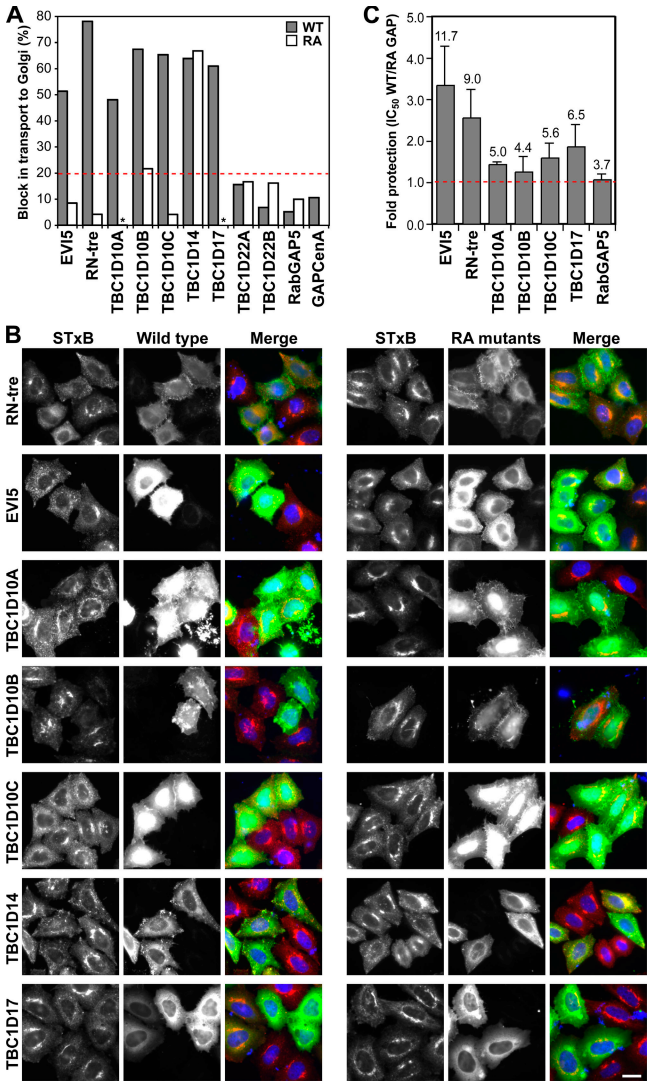

Figure 4. **A subset of human Rab GAPs influence Shiga toxin transport.** (A) Shiga toxin uptake assays were performed on HeLa cells transfected with a library of wild-type human Rab GAPs. Those Rab GAPs showing a block in Shiga toxin uptake were retested as catalytically inactive RA mutants. To measure the extent of Shiga toxin uptake, HeLa cells were transfected with the GFP-tagged wild-type and catalytically inactive mutant GAPs indicated in the figure. These cells were then fixed and stained for a Golgi marker. The percentage of untransfected and transfected cells in which STxB had reached the Golgi was counted for each condition, and the specific reduction in Shiga toxin transport was calculated by subtracting these two figures (transfected − untransfected cells). These numbers are plotted on the bar graph. The dotted red line indicates the cut-off chosen for consideration as a positive. Asterisks indicate that transport was the same as in control cells. (B) Images of the Rab GAPs showing a catalytic activity–dependent block or reduction in Shiga toxin uptake after 60 min. Shiga toxin is in red, transfected Rab GAPs are in green, and DNA is stained blue. (C) Cytotoxicity assays were performed using the Rab GAPs listed in the figure. The IC_{50} of Shiga-like toxin 1 was measured in cells expressing either the wild type (WT) or the catalytically inactive (RA) mutant GAPs. These values were then corrected for transfection efficiency averaging 13.9–18.7%. An increase in the IC_{50} for wild type compared with RA GAPs indicates reduced cytotoxicity, and this is plotted in the graph as the fold protection, with 1 (red dotted line) corresponding to no protection ($n \geq 3$). The corrected IC_{50} values for each condition are shown above each column, and the IC_{50} of empty vector–transfected control cells was 3.5 ng/ml. Error bars represent SD. Bar, 10 μm.

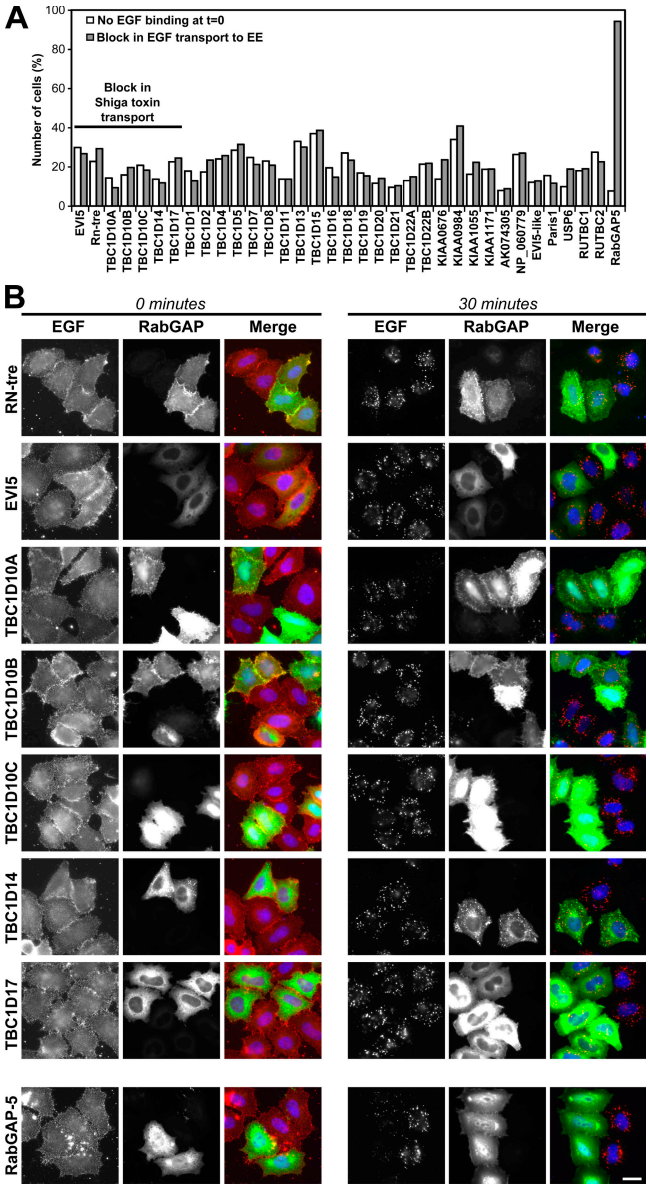

Figure 5. **Rab GAPs altering Shiga toxin transport do not prevent EGF uptake.** (A) EGF uptake assays were performed on HeLa cells transfected with a library of wild-type human Rab GAPs listed in the figure. The number of cells binding and then taking up EGF was counted for each condition. The graph shows cells either failing to bind (open bars) or taking up (closed bars) EGF. (B) EGF uptake assays were performed on HeLa cells transfected with the Rab GAPs capable of blocking Shiga toxin uptake and RabGAP-5. The initially bound EGF at 0 min of transport and the extent of EGF transport at 30 min are shown. EGF is in red, transfected Rab GAPs are in green, and DNA is stained blue. Bar, 10 μm.

Rab5a-c subfamily are substrates for RabGAP-5, whereas Rn-tre acts on Rab43. EVI5 showed strong and specific activity toward Rab35 (>1,200 pmol/h of hydrolyzed GTP), but Rab35 was found to be weakly (sixfold less) activated with several of the GAPs tested here, suggesting that this may be a false positive hit. The substrates of TBC1D10B and TBC1D17 cannot be identified with certainty from the data obtained. Careful analysis of the pattern of GTP hydrolysis suggests that TBC1D10B might act on Rab22a/Rab31, which fall into the same branch of the Rab5 subfamily, whereas TBC1D17 might be a GAP for Rab21 (Fig. 7).

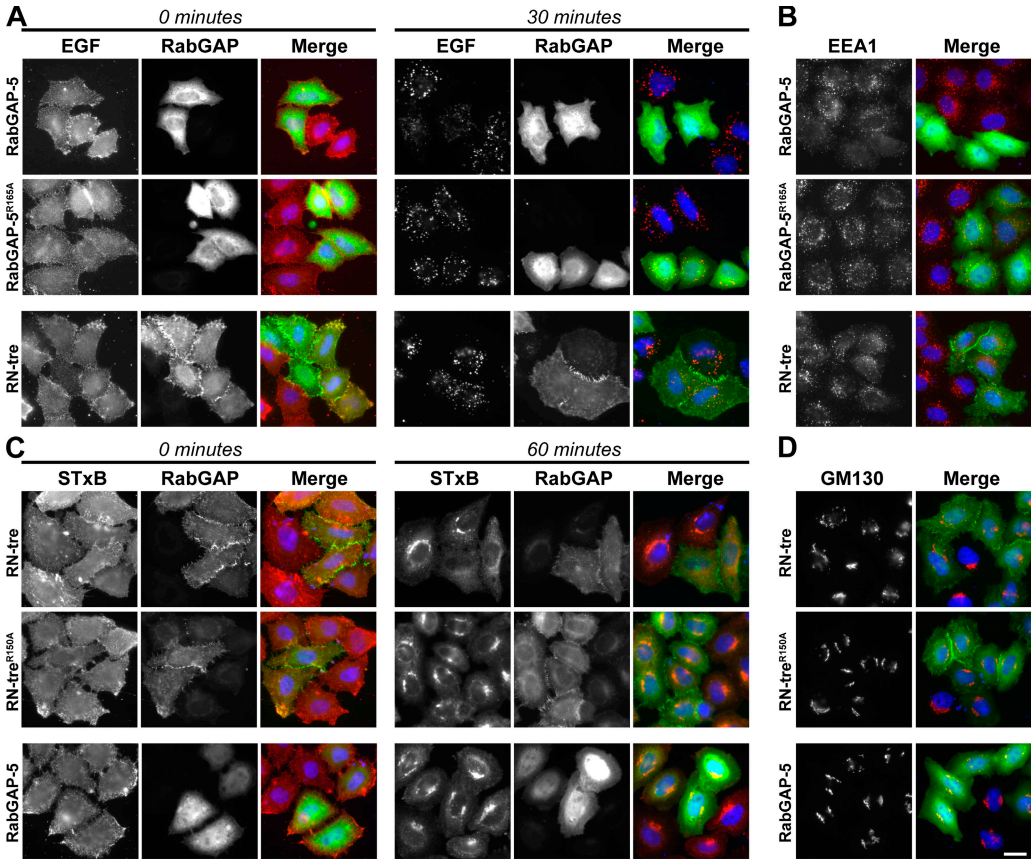

Figure 6. **Discrete Rab GAPs define the Shiga toxin and EGF uptake pathways.** (A and B) HeLa cells were transfected for 24 h with RabGAP-5, the catalytically inactive RabGAP-5^{R165A} mutant, or RN-tre. (A) EGF uptake assays were performed, and the initially bound EGF at 0 min of transport and extent of EGF transport at 30 min are shown in the figure. EGF is in red, and transfected Rab GAPs are in green. (B) The cells were fixed and stained for the transfected Rab GAPs (green) and EEA1 (red). (C and D) HeLa cells were transfected for 24 h with RN-tre, the catalytically inactive RN-tre^{R150A} mutant, or RabGAP-5. (C) Shiga toxin uptake assays were performed, and the initially bound Shiga toxin at 0 min of transport and extent of STxB transport to the Golgi at 60 min are shown. STxB is in red, and transfected Rab GAPs are in green. (D) The cells were fixed and stained for the transfected Rab GAPs (green) and GM130 (red). DNA is stained blue in all panels. Bar, 10 μm.

If the effects of RabGAP-5 on EGF uptake are mediated through Rab5 and those of RN-tre on Shiga toxin transport are mediated through Rab43, cells depleted of these Rabs should display a similar defect to that seen on overexpressing the respective GAP because both conditions reduce the pool of active Rab. In line with this prediction, EEA1 fails to localize to endosomes, and there is a strong reduction in EGF uptake in cells depleted of Rab5 (Fig. 8 A). These cells are still able to transport Shiga toxin to the Golgi apparatus similar to the control cells (Fig. 8 B). In contrast, the Golgi is disorganized, and there is a strong reduction in the transport of Shiga toxin to the Golgi in cells depleted of Rab43 (Fig. 8 C). However, these cells are still able take up EGF similar to the control cells (Fig. 8 D). Consistent with a role for RN-tre and Rab43 in the transport of Shiga toxin to the Golgi apparatus, Rab43 localized to this organelle and showed a staining pattern most similar to the trans-Golgi marker TGN46 (Fig. 8 E). Rab43 showed no overlap with the early endosome marker EEA1 (Fig. 8 E), suggesting that it does not function at early endosomes. Finally, although the siRNA duplexes used were efficient in targeting the appropriate Rab (Fig. S5 A, available at http://www.jcb.org/cgi/content/full/jcb.200612068/DC1), the depletion of Rab21, 22a, 31, and 35 had no clear effects on either Shiga toxin or EGF uptake (unpublished data), and it is therefore unclear whether these Rabs are the targets of the TBC1D10 family of GAPs, TBC1D17, and EVI5. Thus, it will require further investigation to validate the targets of these GAPs.

Together, these observations support two important conclusions. First, RN-tre specifically blocks the Rab43-dependent trafficking of Shiga toxin to the trans-Golgi apparatus, and EGF does not follow this pathway. Second, RabGAP-5 specifically blocks the Rab5-dependent trafficking of EGF through early endosomes, and Shiga toxin does not follow this pathway. Therefore, these two Rab GAPs and their target Rabs define specific trafficking routes for Shiga toxin and EGF.

Discussion

Trafficking pathways can be delineated by Rabs and their GAPs

In this study, we have presented evidence that different sets of Rab GAPs and their target Rabs control specific endocytic trafficking pathways. These results suggest that although the trafficking of Shiga toxin from the cell surface to the Golgi is a

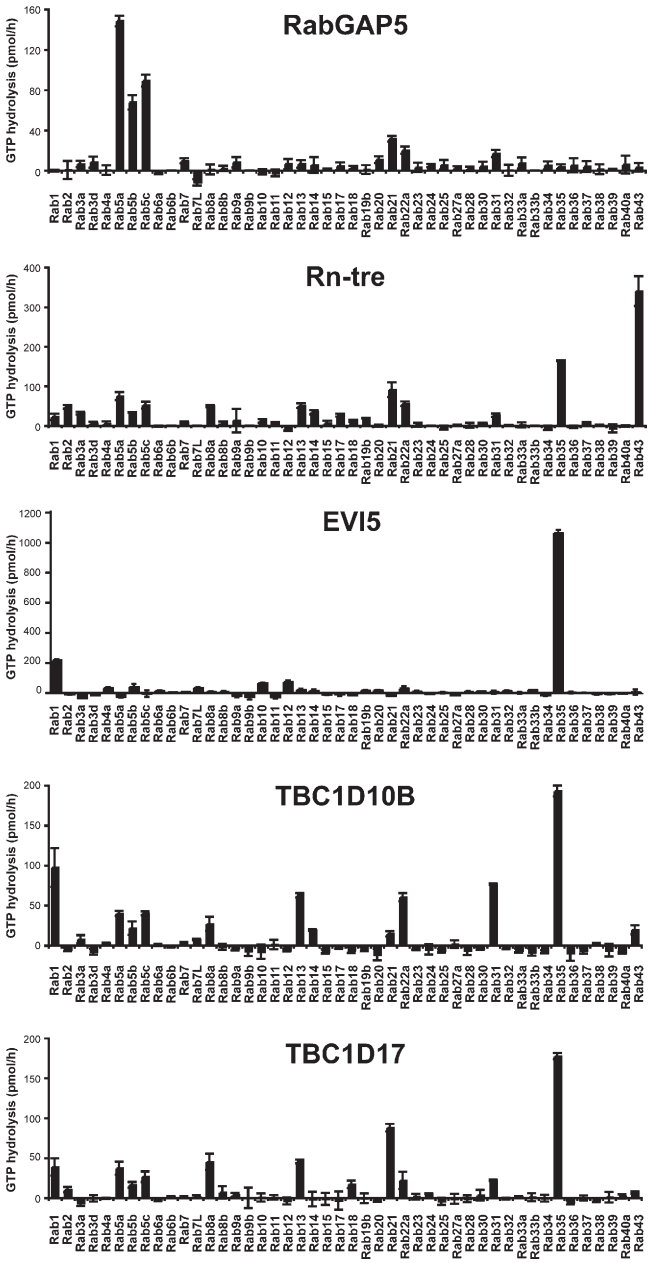

Figure 7. **Biochemical screening for the target Rabs of specific TBC domain proteins.** To determine the specific activity toward a range of GTPases, 0.5 pmol RN-tre, RabGAP-5, TBC1D10B, and TBC1D17 were tested against 100 pmol of the Rab GTPases indicated using the procedures described in Materials and methods. All reactions were performed for 60 min. The basal GTP hydrolysis seen with a buffer control was subtracted for each GTPase, and the mean GTP hydrolysis in picomoles/hour is plotted in the figures. Error bars represent SD.

multistep process dependent on at least six different Rabs and Rab GAPs, EGF trafficking depends only on the action of Rab5 and RabGAP-5. There has been some controversy in the literature concerning the relative importance of RN-tre and RabGAP-5 as regulators for Rab5 and their involvement in the uptake of endocytosed ligands (Lanzetti et al., 2000; Haas et al., 2005). However, the results presented here clearly show that although both of these GAPs are involved in the trafficking of endocytosed ligands, they act on discrete trafficking pathways. One explanation for the differential sensitivity of EGF receptor trafficking to RN-tre could relate to the conditions and cell lines used. With low doses of EGF, the EGF receptor is almost entirely transported via the clathrin-dependent pathway, whereas at higher or saturating doses, it spills over into the clathrin-independent pathway (Sigismund et al., 2005). Thus, with saturating amounts of EGF, RN-tre would be able to prevent transport of the pool of EGF receptor entering via the clathrin-independent pathway. However, our data suggest that this would be a Rab5-independent and Rab43-dependent pathway.

The role of Rab6 in the Shiga toxin trafficking pathway

None of the GAPs capable of blocking Shiga toxin transport was able to cause the release of Bicaudal-D1 from the Golgi to the cytoplasm (Fig. S3), and this indicates that they do not act on Rab6. Why the Rab6 GAP was not found in the screen is unclear, but because the depletion of Rab6 reduces Shiga toxin transport to the Golgi (Fig. 2; Del Nery et al., 2006), this has to be viewed as a false negative. There is evidence that some TBC domain proteins form heterodimeric complexes (Pereira et al., 2001) and that this is necessary for their activity. If this is the case for the Rab6 GAP, it could have been missed in the current screen.

What is clear is that TBC1D11/GAPCenA is unlikely to be the GAP for Rab6. It displays robust biochemical activity toward Rab4 but not Rab6 and has none of the cell biological properties expected for a Rab6 GAP. It cannot block Shiga toxin trafficking or cause release of the Rab6 effector Bicaudal-D1 from the Golgi. Therefore, at this time, the identity of the Rab6 GAP remains mysterious and will require further investigation.

Some cautions on the use of dominant-active Rabs

Some of the results presented here suggest that there are problems with the use of dominant-active GTP-locked Rabs. Although the expression of dominant-active Rab5^{Q79A} results in the trapping of Shiga toxin in an early endocytic compartment, indicating its transport is Rab5 dependent, this interpretation is not supported by the use of specific Rab GAPs. Although RabGAP-5 does block EGF and transferrin trafficking (Haas et al., 2005), it has no effect on the transport of Shiga toxin to the Golgi (Fig. 6). This suggests that although Shiga toxin trafficking is normally Rab5 independent, when dominant-active Rab5 is expressed, it becomes trapped in the enlarged early endocytic compartment created under these conditions (Stenmark et al., 1994). One explanation for this could be that Shiga toxin, although normally trafficking in a Rab5-independent fashion, does pass through a Rab5-positive endocytic compartment, and this can also be perturbed by the overexpression of active mutant forms of Rab5. In contrast, EGF trafficking is blocked by both RabGAP-5 and Rab5^{Q79A} (Figs. 2 and 6) and, therefore, does follow a Rab5-dependent pathway through early endosomes. Thus, dominant-active Rab5 appears to create a situation in which the function of the early endocytic pathway is perturbed such that molecules that normally traffic in a Rab5-independent manner are also affected. Dominant-active Rabs should therefore be used with some caution, and, as shown here,

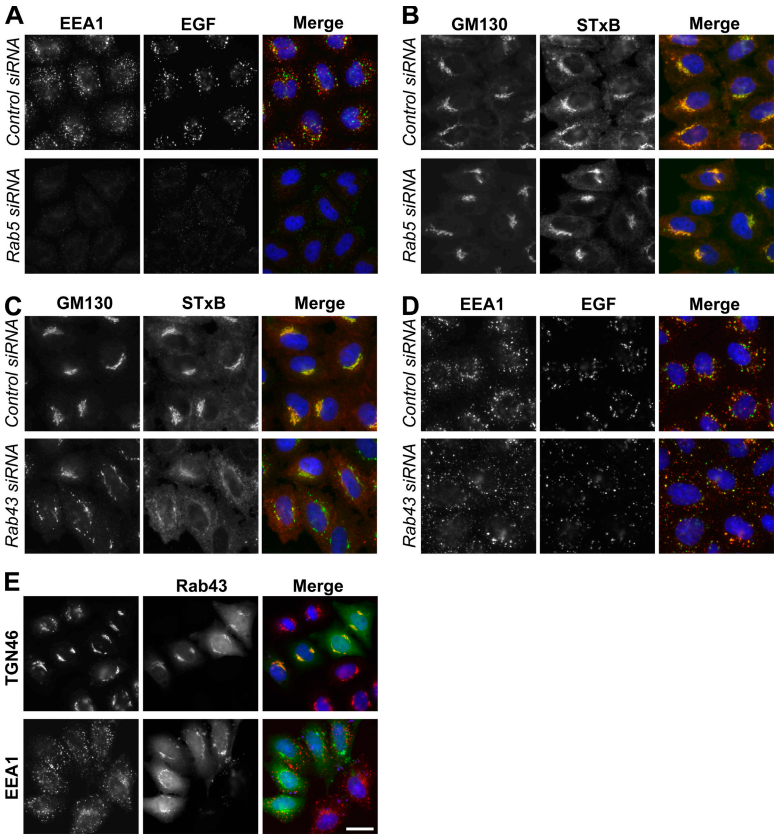

Figure 8. **Functional verification of the targets of RN-tre and RabGAP-5.** (A–D) HeLa cells were transfected with siRNA duplexes to deplete all three isoforms of Rab5 (A and B) or Rab43 (C and D). (A and D) EGF uptake assays were performed, and the extent of EGF transport at 30 min is shown in the figure. EGF is in green, and EEA1 is in red. (B and C) Shiga toxin uptake assays were performed, and the extent of STxB transport to the Golgi at 30 min is shown. STxB is in red, and GM130 is in green. (E) HeLa cells transfected with GFP-tagged Rab43 (green) were fixed after 24 h and stained with antibodies to the Golgi marker TGN46 or the early endosome marker EEA1 (red). DNA is stained blue in all panels. Bar, 10 μm.

specific Rab GAPs provide valuable and specific tools to manipulate the activity of endogenous Rabs.

Are Rab GAPs specific for particular Rab GTPases?

It has been suggested that Rab GAPs are not particularly specific toward their target Rab (Albert and Gallwitz, 1999; Pan et al., 2006). However, this is somewhat counterintuitive because Rabs are argued to be important components acting at specific membrane trafficking steps and for the specification of organelle identity (Pfeffer, 2001; Munro, 2002), and one would therefore expect their regulators to be equally specific. We believe that Rab GAPs are likely to be specific toward particular target Rabs or Rab subfamilies and have several arguments to support this statement. We show that GAPs such as TBC1D11/GAPCenA, RabGAP-5, and RN-tre are highly active toward specific Rabs in biochemical assays. In addition, we can demonstrate that Rab GAPs have highly specific effects on discrete membrane trafficking pathways, which is consistent with the idea that they act on specific Rabs in vivo.

A possible explanation for this discrepancy comes from our investigation of TBC1D11/GAPCenA, which was previously suggested to act on Rab6 (Cuif et al., 1999). In our hands, TBC1D11/GAPCenA acts on Rab4 but not Rab6 and does not have the effects on Rab6 effectors or Shiga toxin transport that is expected for a Rab6 GAP (Fig. 3). Investigation of the interaction between TBC1D11/GAPCenA and Rabs shows that regions outside of the minimal predicted catalytic domain are required for specific Rab binding (Figs. 3 and S1). Strikingly, deletion of these regions relaxes the interaction specificity of the protein. Previous studies have used truncated GAP domains rather than full-length proteins (Albert and Gallwitz, 1999; Pan et al., 2006), and, in light of our findings, this may be problematic because these proteins may have a relaxed specificity and, thus, may be able to accelerate GTP hydrolysis on a broader spectrum of Rabs. An analogous situation has been described for the GAP1 family of bifunctional Ras and Rap GAPs (Kupzig et al., 2006). In this case, regions outside of the core catalytic domain are required for the recognition of Rap (Kupzig et al., 2006). Further investigation of Rab GAP specificity is needed before any general conclusions can be made, but it is clearly important to study the full-length proteins and not only the truncated fragments corresponding to predicted domains.

Understanding Rab GAP function

There are >60 Rab family GTPases encoded by the human genome and at least 39 TBC domain–containing Rab GAPs. However, little is known about the function of the majority of these proteins. This is partly the result of the enormous complexity of membrane trafficking systems and the lack of suitable cell biological models for Rabs with functions in specific tissues. As a first step in unravelling this complex network, we have screened for Rab GAPs that can influence the trafficking of Shiga toxin to the Golgi or of EGF to early endosomes. Using biochemical assays, we have then identified target Rabs for several of these GAPs. This approach should be useful for the study of other trafficking events, for trafficking between the ER and Golgi apparatus, or for a wide variety of different regulated secretory events.

Materials and methods

Antibody reagents

The antibody reagents used were as follows: mouse anti-GM130 and EEA1 (Becton Dickinson), sheep anti-TGN46 (Serotec), rabbit anti-Rab6 (Santa Cruz Biotechnology, Inc.), and Bicaudal-D1 (Short et al., 2002). Donkey secondary antibodies conjugated to HRP, AMCA, CY2, and CY3 were obtained from Jackson ImmunoResearch Laboratories.

Molecular biology and protein expression

The bacterial expression construct for STxB was provided by Y. Misumi (Fukuoka University School of Medicine, Fukuoka, Japan). Human Rab GAPs were identified by searching the GenBank/EMBL/DDBJ database using the TBC domain signature motifs defined by Rak et al. (2000). The human Rab GAPs (EVI-5, RN-tre [USP6NL], RUTBC1, RUTBC2, RabGAP-5 [RUTBC3], TBC1D1, TBC1D2, TBC1D3B, TBC1D4, TBC1D5, TBC1D6, TBC1D7, TBC1D8, TBC1D10A, TBC1D10B, TBC1D10C, TBC1D11 [GAPCenA], TBC1D12, TBC1D13, TBC1D14, TBC1D15, TBC1D16, TBC1D17, TBC1D18, TBC1D19, TBC1D20, TBC1D21, TBC1D22A, TBC1D22B, USP6, AK074305, KIAA1055, KIAA0676, KIAA0882, NP_060222, NP_060779, EVI5-like, KIAA0984, and KIAA1171) were then amplified from either human testis cDNA (Becton Dickinson) or HeLa cDNA using the pfu polymerase (Stratagene) and were cloned in pCRII-TOPO (Invitrogen). Point mutations were introduced using the QuikChange method (Stratagene). Constructs were confirmed by DNA sequencing (Medigenomix; Max Planck Institute biochemistry sequencing core facility). Mammalian expression constructs were made in pcDNA3.1+ (Invitrogen) modified to encode a myc epitope tag and the pEGFP-C2 vector (CLONTECH Laboratories, Inc.). For yeast two-hybrid assays, Rabs were inserted into the bait vector pFBT9, pGBT9 (CLONTECH Laboratories, Inc.) was modified to carry kanamycin resistance, and Rab GAPs and mutants thereof were inserted into the prey vector pACT2 (CLONTECH Laboratories, Inc.). Yeast two-hybrid assays were performed according to the yeast protocol handbook (CLONTECH Laboratories, Inc.) as described previously (Haas et al., 2005). Bacterial expression was performed using the T7 polymerase hexahistidine-GST expression vector pFAT2 for Rabs and the maltose-binding protein expression vector pMalC2 (New England Biolabs, Inc.) for Rab GAPs and the BL21(DE3) and JM109 strains, respectively. Fusion proteins were purified over nickel-nitrilotriacetic acid agarose (QIAGEN) or amylose resin (New England Biolabs, Inc.). Proteins were dialysed overnight against 50 mM Tris-HCl, pH 8.0, 150 mM NaCl, and 2 mM DTT, and aliquots were frozen in liquid nitrogen for storage at –80°C.

GTP hydrolysis assays

For Rab-loading reactions, 10 µl of assay buffer, 73 µl H_2O, 10 µl 10 mM EDTA, pH 8.0, 5 µl of 1 mM GTP, 2 µl γ-[^{32}P]GTP (10 mCi/ml; 5,000 Ci/mmol; GE Healthcare), and 100 pmol Rab protein were mixed on ice. After 15 min of incubation at 30°C, loaded Rabs were stored on ice. GTP binding was measured using a nitrocellulose filter-binding assay (Du and Novick, 2001). GAP reactions were started by the addition of 0.5 pmol Rab GAP as specified in the figures. A 2.5-µl aliquot of the assay mix was scintillation counted to measure the specific activity in counts per minute/picomole GTP. Reactions were then incubated at 30°C, taking 5-µl samples in duplicate at suitable time points as indicated in the figures. The 5-µl aliquots were immediately added to 795 µl of ice-cold 5% [wt/vol] activated charcoal slurry in 50 mM NaH_2PO_4, left for 1 h on ice, and centrifuged at 16,100 *g* in a benchtop microfuge (5417R; Eppendorf) to pellet the charcoal. A 400-µl aliquot of the supernatant was scintillation counted, and the amount of GTP hydrolyzed was calculated from the specific activity of the reaction mixture.

Cell culture and RNAi

HeLa cells were cultured at 37°C and 5% CO_2 in growth medium (DME containing 10% FCS). HeLa cells plated on glass coverslips in a six-well plate at a density of 70,000 cells/well were used for plasmid transfection and at 25,000 cells/well for RNAi using conditions that were described previously (Haas et al., 2005). Rabs were targeted using siRNA duplexes obtained from Dharmacon. The sequences are listed in Fig. S5 B. For Western blotting, cells from three wells of a six-well plate were washed in 2 ml PBS and lysed in 70–80 µl of 50 mM Tris-HCl, pH 7.4, 150 mM NaCl, and 0.1% [wt/vol] Triton X-100. For each lane of a minigel, 10 µg of the protein lysate was loaded.

Shiga-like toxin cytotoxicity assays

Cytotoxicity was defined as a decrease in the ability of cells to incorporate [^{35}S]methionine into acid-precipitable material after Shiga-like toxin 1 treatment using an established method (Spooner et al., 2004). HeLa cells were transiently transfected with either wild-type or RA mutant Rab GAPs for 9 h using Fugene-6 and the manufacturer's protocol (Roche Diagnostics) and were replated in 96-well plates at a density of 1.5×10^4 cells/well and left for another 15 h. After washing with PBS, cells were incubated for 1 h with 100 µl DME/FCS containing serial twofold dilutions from 0.05–50 ng/ml Shiga-like toxin 1. Subsequently, cells were washed with PBS and incubated in PBS containing 50 µCi/ml [^{35}S]methionine for 30 min. Labeled proteins were precipitated with three washes in 5% [wt/vol] trichloroacetic acid, the wells were washed twice with PBS, 50 µl of scintillation fluid was added, and the amount of radiolabel incorporated was then determined in a counter (MicroBeta 1450 TriLux; PerkinElmer). For each condition, the IC_{50} for Shiga-like toxin 1 was calculated from the toxin titration performed in triplicate.

EGF uptake assays

EGF coupled to 200 µg/ml AlexaFluor488 or -555 (40× stock; Invitrogen) were stored as stock solutions in PBS at –20°C. For uptake assays, HeLa cells plated on glass coverslips at a density of 70,000 cells/well of a six-well plate were washed three times with serum-free growth medium 36 h after plating and were incubated in serum-free growth medium for 15–16 h at 37°C and 5% CO_2. Coverslips were then washed three times in ice-cold PBS and placed on 40-µl drops of uptake medium (DME, 2% [wt/vol] BSA, and 20 mM Hepes-NaOH, pH 7.5) and 5 µg/ml EGF on an ice-cold metal plate covered in Parafilm (Pechiney Plastic Packaging). After 30 min of incubation, the coverslips were washed three times in ice-cold PBS to remove excess ligand. One coverslip was fixed to give the total bound ligand, whereas the remaining coverslips were transferred to a six-well plate containing prewarmed growth medium and were incubated at 37°C and 5% CO_2. At the time points indicated in the figures, coverslips were fixed and processed for immunofluorescence microscopy.

Preparation of STxB and uptake assays

Recombinant STxB was prepared as described previously (Johannes et al., 1997; Sohda et al., 2005) and labeled on amine residues for 5 min at room temperature with an *N*-hydroxysuccinimidyl ester of Cy3 according to the manufacturer's instructions (GE Healthcare). These conditions lead to a stoichiometry of five Cy3 dye molecules per pentamer of STxB. The cell line and conditions used for uptake assays were the same as those described for EGF except that 0.7 µg/ml Cy3-STxB were used. For combined EGF and STxB assays, both proteins were mixed and bound simultaneously to the cell surface, and the standard procedure was followed.

Image acquisition

Cells to be imaged were fixed for 20 min in 3% [wt/vol] PFA, quenched for 10 min with 50 mM ammonium chloride, and permeabilized with 0.1% [vol/vol] Triton X-100 for 5 min to allow labeling of internal cell structures. For cell surface labeling, cells were not permeabilized. All solutions were made in PBS, and antibody staining was performed for 60 min using a 1,000-fold dilution of antiserum or purified antibody at a final concentration of 1 µg/ml. Coverslips were mounted in 10% [wt/vol] Moviol 4-88, 1 µg/ml DAPI, and 25% [wt/vol] glycerol in PBS. Images were collected at a room temperature of 22°C using a microscope (Axioskop-2; Carl Zeiss MicroImaging, Inc.) with a 63× plan Apochromat oil immersion objective (Carl Zeiss MicroImaging, Inc.) of NA 1.4, standard filter sets (Carl Zeiss MicroImaging, Inc.), a 1,300 × 1,030-pixel cooled CCD camera (CCD-1300-Y; Princeton Instruments), and Metavue software (Visitron Systems). Images were cropped in Photoshop 7.0 (Adobe) or CS2 software (Adobe) without contrast or other adjustments, sized, and placed using Illustrator 11.0 (Adobe) or CS2.

Online supplemental material

Fig. S1 shows that the interaction specificity of TBC1D11/GAPCenA with human Rab GTPases involves regions outside of the TBC domain. Fig. S2 shows the effect of Rab GAPs blocking Shiga toxin uptake on Golgi morphology. Fig. S3 shows the effect of Rab GAPs blocking Shiga toxin uptake on the Rab6 effector Bicaudal-D1. Fig. S4 shows that RabGAP-5 interacts with Rab5A-C but not other Rabs. Fig. S5 shows the specific depletion of target Rabs using RNAi. Online supplemental material is available at http://www.jcb.org/cgi/content/full/jcb.200612068/DC1.

We would like to thank Dr. Y. Misumi (Fukuoka University School of Medicine, Fukuoka, Japan) for providing reagents and protocols for the purification of STxB, Dr. A. Uldschmid for help with column chromatography and purification of STxB, and Robert Kopajtich for technical assistance.

This work was supported by the Max Planck Society and the Deutsche Forschungsgemeinschaft (group of F.A. Barr). Work at the University of Warwick was supported by the National Institutes of Health grant 5 U01AI 65869.

Submitted: 13 December 2006
Accepted: 17 May 2007

References

Ahmadian, M.R., P. Stege, K. Scheffzek, and A. Wittinghofer. 1997. Confirmation of the arginine-finger hypothesis for the GAP-stimulated GTP-hydrolysis reaction of Ras. *Nat. Struct. Biol.* 4:686–689.

Albert, S., and D. Gallwitz. 1999. Two new members of a family of Ypt/Rab GTPase activating proteins. Promiscuity of substrate recognition. *J. Biol. Chem.* 274:33186–33189.

Albert, S., E. Will, and D. Gallwitz. 1999. Identification of the catalytic domains and their functionally critical arginine residues of two yeast GTPase-activating proteins specific for Ypt/Rab transport GTPases. *EMBO J.* 18:5216–5225.

Bonifacino, J.S., and R. Rojas. 2006. Retrograde transport from endosomes to the trans-Golgi network. *Nat. Rev. Mol. Cell Biol.* 7:568–579.

Choudhury, R., A. Diao, F. Zhang, E. Eisenberg, A. Saint-Pol, C. Williams, A. Konstantakopoulos, J. Lucocq, L. Johannes, C. Rabouille, et al. 2005. Lowe syndrome protein OCRL1 interacts with clathrin and regulates protein trafficking between endosomes and the trans-Golgi network. *Mol. Biol. Cell*. 16:3467–3479.

Cuif, M.H., F. Possmayer, H. Zander, N. Bordes, F. Jollivet, A. Couedel-Courteille, I. Janoueix-Lerosey, G. Langsley, M. Bornens, and B. Goud. 1999. Characterization of GAPCenA, a GTPase activating protein for Rab6, part of which associates with the centrosome. *EMBO J.* 18:1772–1782.

Del Nery, E., S. Miserey-Lenkei, T. Falguieres, C. Nizak, L. Johannes, F. Perez, and B. Goud. 2006. Rab6A and Rab6A' GTPases play non-overlapping roles in membrane trafficking. *Traffic*. 7:394–407.

Du, L.L., and P. Novick. 2001. Purification and properties of a GTPase-activating protein for yeast Rab GTPases. *Methods Enzymol.* 329:91–99.

Girod, A., B. Storrie, J.C. Simpson, L. Johannes, B. Goud, L.M. Roberts, J.M. Lord, T. Nilsson, and R. Pepperkok. 1999. Evidence for a COP-I-independent transport route from the Golgi complex to the endoplasmic reticulum. *Nat. Cell Biol.* 1:423–430.

Haas, A.K., E. Fuchs, R. Kopajtich, and F.A. Barr. 2005. A GTPase-activating protein controls Rab5 function in endocytic trafficking. *Nat. Cell Biol.* 7:887–893.

Hyvola, N., A. Diao, E. McKenzie, A. Skippen, S. Cockcroft, and M. Lowe. 2006. Membrane targeting and activation of the Lowe syndrome protein OCRL1 by rab GTPases. *EMBO J*. 25:3750–3761.

Johannes, L., and B. Goud. 1998. Surfing on a retrograde wave: how does Shiga toxin reach the endoplasmic reticulum? *Trends Cell Biol.* 8:158–162.

Johannes, L., and B. Goud. 2000. Facing inward from compartment shores: how many pathways were we looking for? *Traffic*. 1:119–123.

Johannes, L., D. Tenza, C. Antony, and B. Goud. 1997. Retrograde transport of KDEL-bearing B-fragment of Shiga toxin. *J. Biol. Chem.* 272:19554–19561.

Kupzig, S., D. Deaconescu, D. Bouyoucef, S.A. Walker, Q. Liu, C.L. Polte, O. Daumke, T. Ishizaki, P.J. Lockyer, A. Wittinghofer, and P.J. Cullen. 2006. GAP1 family members constitute bifunctional Ras and Rap GTPase-activating proteins. *J. Biol. Chem.* 281:9891–9900.

Lanzetti, L., V. Rybin, M.G. Malabarba, S. Christoforidis, G. Scita, M. Zerial, and P.P. Di Fiore. 2000. The Eps8 protein coordinates EGF receptor signalling through Rac and trafficking through Rab5. *Nature*. 408:374–377.

Lauvrak, S.U., M.L. Torgersen, and K. Sandvig. 2004. Efficient endosome-to-Golgi transport of Shiga toxin is dependent on dynamin and clathrin. *J. Cell Sci.* 117:2321–2331.

Lu, L., G. Tai, and W. Hong. 2004. Autoantigen Golgin-97, an effector of Arl1 GTPase, participates in traffic from the endosome to the trans-golgi network. *Mol. Biol. Cell*. 15:4426–4443.

Mallard, F., C. Antony, D. Tenza, J. Salamero, B. Goud, and L. Johannes. 1998. Direct pathway from early/recycling endosomes to the Golgi apparatus revealed through the study of shiga toxin B-fragment transport. *J. Cell Biol.* 143:973–990.

Mallard, F., B.L. Tang, T. Galli, D. Tenza, A. Saint-Pol, X. Yue, C. Antony, W. Hong, B. Goud, and L. Johannes. 2002. Early/recycling endosomes-to-TGN transport involves two SNARE complexes and a Rab6 isoform. *J. Cell Biol.* 156:653–664.

Matanis, T., A. Akhmanova, P. Wulf, E. Del Nery, T. Weide, T. Stepanova, N. Galjart, F. Grosveld, B. Goud, C.I. De Zeeuw, et al. 2002. Bicaudal-D regulates COPI-independent Golgi-ER transport by recruiting the dynein-dynactin motor complex. *Nat. Cell Biol.* 4:986–992.

Monier, S., F. Jollivet, I. Janoueix-Lerosey, L. Johannes, and B. Goud. 2002. Characterization of novel Rab6-interacting proteins involved in endosome-to-TGN transport. *Traffic*. 3:289–297.

Munro, S. 2002. Organelle identity and the targeting of peripheral membrane proteins. *Curr. Opin. Cell Biol.* 14:506–514.

Nichols, B.J., A.K. Kenworthy, R.S. Polishchuk, R. Lodge, T.H. Roberts, K. Hirschberg, R.D. Phair, and J. Lippincott-Schwartz. 2001. Rapid cycling of lipid raft markers between the cell surface and Golgi complex. *J. Cell Biol.* 153:529–541.

Niyogi, S.K. 2005. Shigellosis. *J. Microbiol.* 43:133–143.

O'Loughlin, E.V., and R.M. Robins-Browne. 2001. Effect of Shiga toxin and Shiga-like toxins on eukaryotic cells. *Microbes Infect.* 3:493–507.

Pan, X., S. Eathiraj, M. Munson, and D.G. Lambright. 2006. TBC-domain GAPs for Rab GTPases accelerate GTP hydrolysis by a dual-finger mechanism. *Nature*. 442:303–306.

Pereira, G., T.U. Tanaka, K. Nasmyth, and E. Schiebel. 2001. Modes of spindle pole body inheritance and segregation of the Bfa1p-Bub2p checkpoint protein complex. *EMBO J.* 20:6359–6370.

Pfeffer, S.R. 2001. Rab GTPases: specifying and deciphering organelle identity and function. *Trends Cell Biol.* 11:487–491.

Rak, A., R. Fedorov, K. Alexandrov, S. Albert, R.S. Goody, D. Gallwitz, and A.J. Scheidig. 2000. Crystal structure of the GAP domain of Gyp1p: first insights into interaction with Ypt/Rab proteins. *EMBO J.* 19:5105–5113.

Sandvig, K., and B. van Deurs. 2002. Membrane traffic exploited by protein toxins. *Annu. Rev. Cell Dev. Biol.* 18:1–24.

Sandvig, K., S. Olsnes, J.E. Brown, O.W. Petersen, and B. van Deurs. 1989. Endocytosis from coated pits of Shiga toxin: a glycolipid-binding protein from *Shigella dysenteriae* 1. *J. Cell Biol.* 108:1331–1343.

Sandvig, K., O. Garred, K. Prydz, J.V. Kozlov, S.H. Hansen, and B. van Deurs. 1992. Retrograde transport of endocytosed Shiga toxin to the endoplasmic reticulum. *Nature*. 358:510–512.

Short, B., C. Preisinger, J. Schaletzky, R. Kopajtich, and F.A. Barr. 2002. The Rab6 GTPase regulates recruitment of the dynactin complex to Golgi membranes. *Curr. Biol.* 12:1792–1795.

Sigismund, S., T. Woelk, C. Puri, E. Maspero, C. Tacchetti, P. Transidico, P.P. Di Fiore, and S. Polo. 2005. Clathrin-independent endocytosis of ubiquitinated cargos. *Proc. Natl. Acad. Sci. USA*. 102:2760–2765.

Sohda, M., Y. Misumi, S. Yoshimura, N. Nakamura, T. Fusano, S. Sakisaka, S. Ogata, J. Fujimoto, N. Kiyokawa, and Y. Ikehara. 2005. Depletion of vesicle-tethering factor p115 causes mini-stacked Golgi fragments with delayed protein transport. *Biochem. Biophys. Res. Commun.* 338:1268–1274.

Spooner, R.A., P.D. Watson, C.J. Marsden, D.C. Smith, K.A. Moore, J.P. Cook, J.M. Lord, and L.M. Roberts. 2004. Protein disulphide-isomerase reduces ricin to its A and B chains in the endoplasmic reticulum. *Biochem. J.* 383:285–293.

Spooner, R.A., D.C. Smith, A.J. Easton, L.M. Roberts, and J.M. Lord. 2006. Retrograde transport pathways utilised by viruses and protein toxins. *Virol. J.* 3:26.

Stenmark, H., R.G. Parton, O. Steele-Mortimer, A. Lutcke, J. Gruenberg, and M. Zerial. 1994. Inhibition of rab5 GTPase activity stimulates membrane fusion in endocytosis. *EMBO J.* 13:1287–1296.

Strom, M., P. Vollmer, T.J. Tan, and D. Gallwitz. 1993. A yeast GTPase-activating protein that interacts specifically with a member of the Ypt/Rab family. *Nature*. 361:736–739.

Tai, G., L. Lu, T.L. Wang, B.L. Tang, B. Goud, L. Johannes, and W. Hong. 2004. Participation of the syntaxin 5/Ykt6/GS28/GS15 SNARE complex in transport from the early/recycling endosome to the trans-Golgi network. *Mol. Biol. Cell*. 15:4011–4022.

White, J., L. Johannes, F. Mallard, A. Girod, S. Grill, S. Reinsch, P. Keller, B. Tzschaschel, A. Echard, B. Goud, and E.H. Stelzer. 1999. Rab6 coordinates a novel Golgi to ER retrograde transport pathway in live cells. *J. Cell Biol.* 147:743–760.

Zerial, M., and H. McBride. 2001. Rab proteins as membrane organizers. *Nat. Rev. Mol. Cell Biol.* 2:107–117.